

Correspondence

In Vitro and In Vivo Tissue Harmonic Images Obtained With Parallel Transmit Beamforming by Means of Orthogonal Frequency Division Multiplexing

Libertario Demi, Alessandro Ramalli, Gabriele Giannini,
and Massimo Mischi

Abstract—In classic pulse-echo ultrasound imaging, the data acquisition rate is limited by the speed of sound. To overcome this, parallel beamforming techniques in transmit (PBT) and in receive (PBR) mode have been proposed. In particular, PBT techniques, based on the transmission of focused beams, are more suitable for harmonic imaging because they are capable of generating stronger harmonics. Recently, orthogonal frequency division multiplexing (OFDM) has been investigated as a means to obtain parallel beamformed tissue harmonic images. To date, only numerical studies and experiments in water have been performed, hence neglecting the effect of frequency-dependent absorption. Here we present the first *in vitro* and *in vivo* tissue harmonic images obtained with PBT by means of OFDM, and we compare the results with classic B-mode tissue harmonic imaging. The resulting contrast-to-noise ratio, here used as a performance metric, is comparable. A reduction by 2 dB is observed for the case in which three parallel lines are reconstructed. In conclusion, the applicability of this technique to ultrasonography as a means to improve the data acquisition rate is confirmed.

I. INTRODUCTION

PHYSICALLY, the speed of sound in human tissue limits the achievable data acquisition rate of classic pulse-echo imaging. To go beyond this limit, different parallel beamforming techniques have been developed, which can be applied to, e.g., three-dimensional ultrasound imaging so as to attain a higher volume rate [1], [2]. These techniques can be divided into two categories: parallel beamforming in reception (PBR) and transmission (PBT). PBR techniques [3]–[7] employ a wide beam or a plane wave in transmission to insonify a large volume and, when receiving, several image lines may be formed in parallel. Consequently, PBR techniques are not suitable for performing harmonic imaging. Employing a wide beam or plane wave in transmission results, in fact, in lower pressure amplitudes, compared with focused ultrasound beams, and conflicts with the required high-pressure fields necessary for the formation of the harmonic components. Unlike PBR, PBT techniques may be more easily applied to attain har-

monic imaging at higher data acquisition rate, because focused parallel beams may be used in transmission to increase the amplitude of the generated pressure wave fields.

Harmonic imaging, compared with fundamental imaging, improves the image resolution (in the axial, lateral, and elevation directions), and reduces the effects of clutter, side lobes, and grating lobes [8]–[12], ultimately reducing the influence of the related artifacts, thus improving the image contrast.

When implementing PBT, a possible approach is to spatially distribute the transmitted beams over the volume of interest [13]–[15], and to employ combinations of transmit and receive apodizations [13] or beam transformation techniques [16] to reduce the interbeam interference. Recently, an alternative solution based on orthogonal frequency division multiplexing (OFDM) was presented [17]. With this technique, multiple beams are generated by allocating a portion of the available transducer bandwidth to each beam. Multiple image lines can thus be formed in parallel: first, the different beams are directed in different directions; then, in receive, different band-pass filters are applied to extract the echo signals belonging to each direction. Numerical studies show the ability of PBT by means of OFDM to reduce the presence of side lobes. In addition, it increases the amplitude of the main beam compared with PBR [17], increasing the achievable penetration depth. As a drawback, employing narrow bandwidth pulses implies a reduction of the achievable axial resolution. This is, however, counterbalanced by the intrinsic improvement in axial resolution achieved by harmonic imaging [18]. To date, only numerical and *in vitro* studies in water have been reported [17], [19]. In this paper, tissue harmonic images, i.e., ultrasound images based on the scattering of the second-harmonic component, of agarose phantoms and carotid artery obtained with PBT by means of OFDM are shown and compared with those obtained with classic B-mode imaging.

II. METHODOLOGY

Classic B-mode and parallel beamformed tissue harmonic images were obtained employing the LA533 linear array (Esaote, Firenze, Italy) probe. This array consists of 192 elements, each 0.215 mm by 6 mm in size. The pitch is 0.245 mm. The array was connected to the ULA-OP system [20]. An active aperture of 62 elements was used both in transmit and receive. In transmit, the focus was set at 25 mm and a Hanning apodization was used. No steering was applied. In receive, dynamic focusing and apodization (*f*-number = 2) were used. The active aperture was linearly shifted over the array to create a 129-line image. Table I lists the different settings for the different acquisitions performed in this study. When classic B-mode

Manuscript received June 27, 2014; accepted October 18, 2014.

L. Demi and M. Mischi are with the Laboratory of Biomedical Diagnostics, Eindhoven University of Technology, Eindhoven, The Netherlands (e-mail: l.demi@tue.nl).

A. Ramalli and G. Giannini are with the Laboratory of Microelectronics Systems Design, Università degli Studi di Firenze, Florence, Italy.

DOI <http://dx.doi.org/10.1109/TUFFC.2014.006599>

TABLE I. SETTINGS UTILIZED FOR THE DIFFERENT ACQUISITIONS.

Modality	Number of parallel lines	Center frequencies [MHz]	Pulse length [μs]	Band-pass filters bandwidth [MHz]
Standard B-mode (<i>in vitro</i> and <i>in vivo</i>)	1	5.5	0.8	3.6
OFDM PBT (<i>in vitro</i>)	1	5.5	3	1.4
OFDM PBT (<i>in vitro</i>)	2	5 and 6	3	1.4
OFDM PBT (<i>in vitro</i>)	3	4.5, 5.5, and 6.5	3	1.4
OFDM PBT (<i>in vivo</i>)	2	4.75 and 6	2.5	1.7

was applied, each line was formed sequentially and a 0.8 μs flat-top window pulse with a center frequency equal to 5.5 MHz was used. Classic B-mode images were used as reference to evaluate PBT by means of OFDM images.

A. Agarose Phantom Images

An agarose phantom [21] containing cylindrical cavities of different radius, approximately equal to 1, 2.5, and 7 mm, respectively, was used for imaging. When PBT by means of OFDM was applied, 3 μs Gaussian pulses were used as to allow a maximum of three beams to be transmitted in parallel without significant frequency overlap [19]. Images using one, two, or three beams were generated. Even if there is no gain in frame rate achieved, an acquisition using a single beam was performed to evaluate the images as obtained when narrowband pulses are used, and to compare them with classic B-mode imaging. In cases in which two or three beams were transmitted, two or three lines were formed in parallel, respectively. The employed center frequencies were 5.5 MHz; 5 and 6 MHz; or 4.5, 5.5, and 6.5 MHz in cases in which one, two, or three beams were transmitted. An interbeam time delay of 3 μs was applied to avoid the formation of unwanted mixing frequencies and in general to prevent signals from overlapping in time during transmission. Note that the interbeam time delay and the number of image lines formed in parallel increase the length of the transmission phase. Thus, because the reception phase cannot start before the end of the transmission, interbeam delays cause a deeper blind region compared with classic B-mode; the reader is referred to [17] and [19] for details. In our particular case, the blind region extends to 15 mm when reconstructing three lines in parallel. Fig. 1 depicts a schematic of the transmission events for PBT by means of OFDM and classic B-mode, respectively. Both for classic B-mode and PBT, a 5.5 dB/cm time-gain compensation (TGC) was applied. To extract the echoes of the second-harmonic component, seventh-order Butterworth band-pass filters centered at twice the transmitted center frequencies were utilized. However, a depth-dependent center frequency could also be applied because attenuation increases both with depth and frequency. Bandwidths of 3.6 MHz and 1.4 MHz were used for classic B-mode and PBT, respectively. After filtering, the envelope was obtained using the Hilbert transform. As performance metrics, after image formation, the contrast-to-noise ratio (CNR) was calculated [22] for the different cavities as

$$\text{CNR} = 10 \log_{10} \left[\frac{\left(\frac{1}{N_{\text{out}}} \sum a_{\text{out}} - \frac{1}{N_{\text{in}}} \sum a_{\text{in}} \right)^2}{\frac{\sigma_{\text{out}}^2 + \sigma_{\text{in}}^2}{2}} \right], \quad (1)$$

where a_{out} and a_{in} , are the amplitude values in linear scale, N_{out} and N_{in} are the number of points outside and inside the cavity, and σ_{out} and σ_{in} are the standard deviations outside and inside the cavity, respectively. The contours of the cavities were selected by manually overlaying a circle on the ultrasound image. The area outside a cavity was defined as the area between the contour of the cavity and a concentric circle with a radius equal to 2, 5, and 9 mm, respectively, for the small, medium, and large cavities.

B. In Vivo Images

Carotid artery tissue harmonic images of a healthy volunteer were obtained for classic B-mode and PBT. For PBT by means of OFDM, a tissue harmonic image forming two image lines in parallel was made. 2.5-μs Gaussian pulses were used. The two transmitted center frequencies were 4.75 and 6 MHz, respectively. Only two image lines were acquired in parallel for the *in vivo* case because the quality of the image obtained with a higher number of parallel beams was too poor, mainly because of higher interbeam interference compared with the *in vitro* results. Reducing the number of lines acquired in parallel, however, permitted the use of shorter pulses, hence improv-

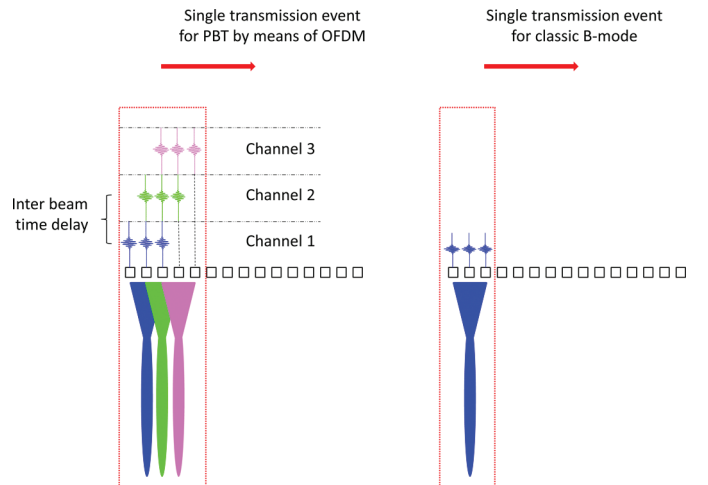


Fig. 1. Schematic representation of the implementation PBT by means of OFDM and classic B-mode for a linear array.

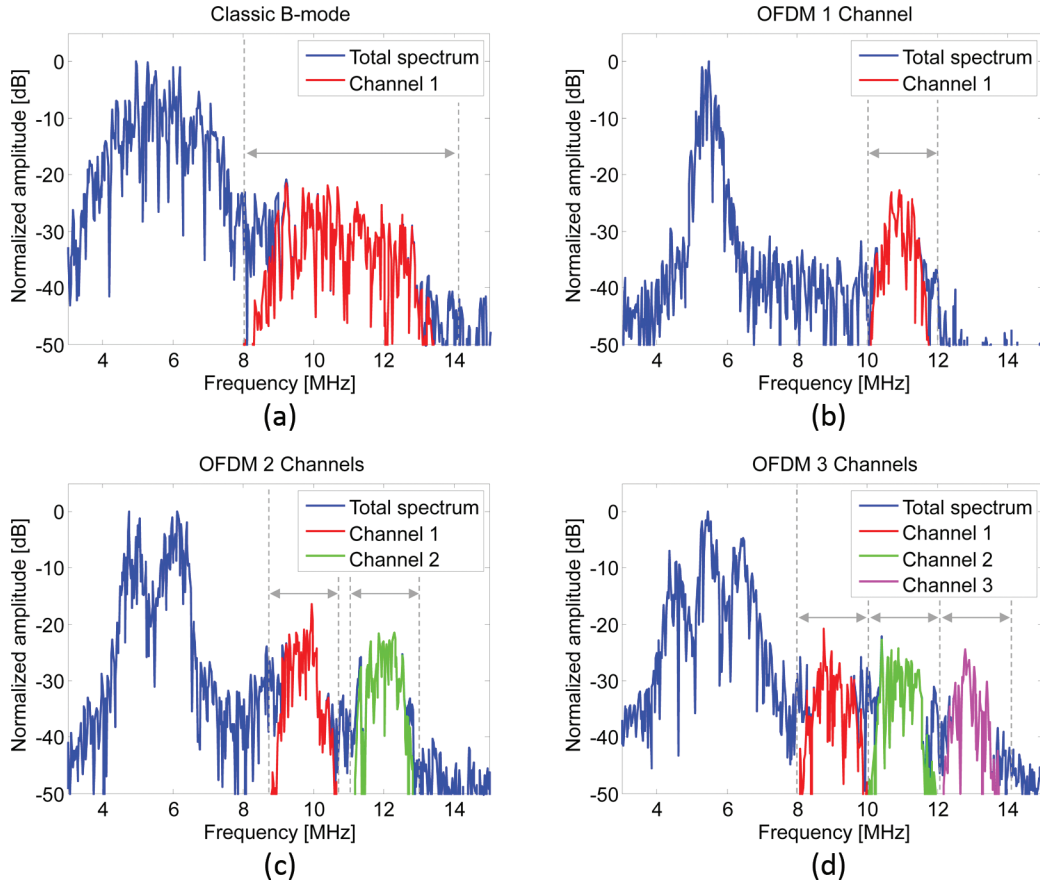


Fig. 2. Received frequency spectrum as obtained with (a) classic B-mode and parallel beamforming by means of OFDM with (b) one, (c) two, and (d) three channels. The receive bandwidths are indicated by gray arrows. These plots are obtained from the RF signals used to form the first line of the corresponding harmonic images displayed in Fig. 3.

ing the axial resolution. Furthermore, it reduces the blind region to 10 mm. An interbeam time delay of 3 μ s was applied. After receiving, a 5.5 dB/cm TGC was applied, and seventh-order Butterworth band-pass filters with a 1.7 MHz bandwidth, centered at twice the transmitted center frequencies, were utilized to select the echoes of the second-harmonic components. After filtering, the envelope was obtained using the Hilbert transform.

III. RESULTS

Fig. 2 shows the received frequency spectrum as obtained from the agarose phantom experiment with (a) classic B-mode, and PBT by means of OFDM with (b) one, (c) two, and (d) three channels. As can be observed from the spectra, the transducer bandwidth was divided into two main sub-bands: the fundamental component band, from 4 to 7 MHz, and the second harmonic band, from 8 to 14 MHz. Both for (a) classic B-mode and (d) PBT with three channels, these two bandwidths were fully utilized. Fig. 3 shows the tissue harmonic image of the agarose phantom as obtained with (a) classic B-mode and PBT by means of OFDM with (b) one, (c) two, and (d) three channels. A 20 dB dynamic range is shown. Two main differences can be noted when comparing classic B-

mode images with PBT images: 1) A loss in axial resolution is observable in PBT images; and 2) the speckle pattern changes for increasing number of channels, deforming from standard to stripe-like speckle pattern. Using a narrowband pulse degrades the axial resolution of the final image. Consequently, the speckle pattern will also deform in the axial direction, as is visible in Fig. 3(b) when compared with Fig. 3(a). Furthermore, when narrowband pulses with different center frequencies are used, the speckle pattern shows a deformation also in the lateral direction. This is best appreciable in the images Figs. 3(c) and 3(d), after the focus (25 mm). Fig. 4 shows the same tissue harmonic images after a two-dimensional 1.4 mm by 1.4 mm rotationally symmetric Gaussian low-pass spatial filter was applied. The filter was applied after envelope detection and the same filter has been applied to all images. A 20 dB dynamic range is shown. Fig. 5 shows the CNR values as obtained for the different cavities with classic B-mode, and PBT by means of OFDM with one, two, and three channels. For the 2.5-mm-radius cavity, the deepest cavity (see Figs. 3 and 4) has been used to evaluate the CNR. Results before and after spatial filtering are shown. Overall, filtering improves CNR. Comparable CNR values are shown among the different images. Fig. 6 shows the carotid artery tissue harmonic image as obtained with (a) classic B-mode, and (b) parallel beamforming by means

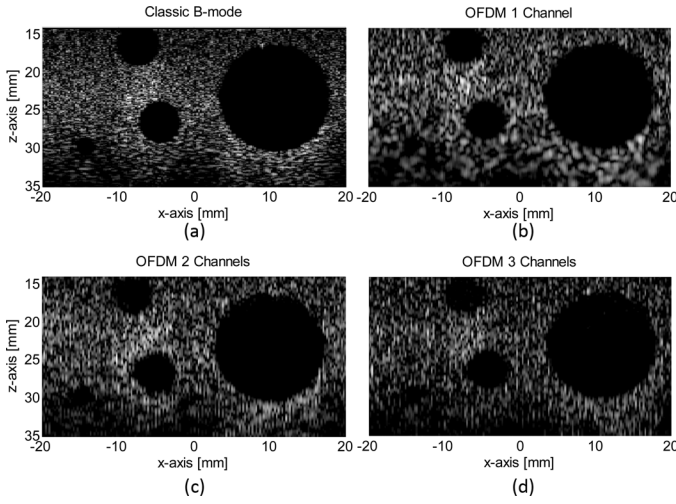


Fig. 3. Agarose phantom tissue harmonic image as obtained with (a) classic B-mode and parallel beamforming by means of OFDM with (b) one, (c) two, and (d) three channels. No spatial filtering applied. A 20-dB dynamic range is shown.

of OFDM. A 20 dB dynamic range is shown. The same spatial filtering introduced for the phantom experiment was applied.

IV. DISCUSSION

In this paper, PBT by means of OFDM tissue harmonic images obtained from a phantom and *in vivo* are presented. When comparing them with the corresponding classic B-mode tissue harmonic images, several aspects can be pointed out:

- 1) Although extensively addressed in [19], it is still worth noting that applying narrowband pulses for

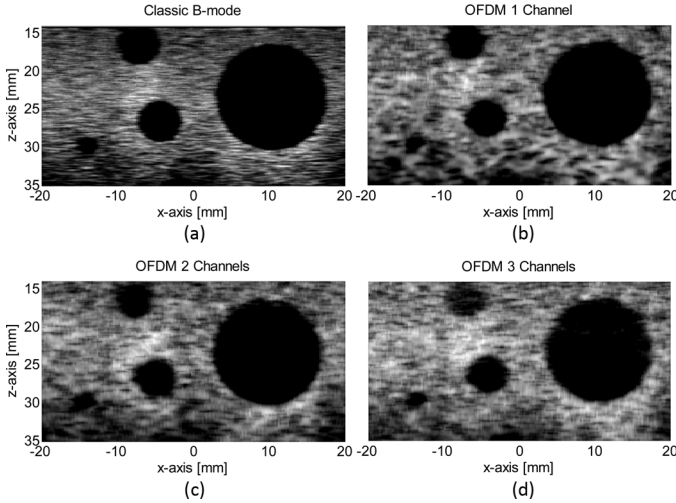


Fig. 4. Agarose phantom tissue harmonic image as obtained with (a) classic B-mode and parallel beamforming by means of OFDM with (b) one, (c) two, and (d) three channels. Spatial filtering applied. A 20-dB dynamic range is shown.

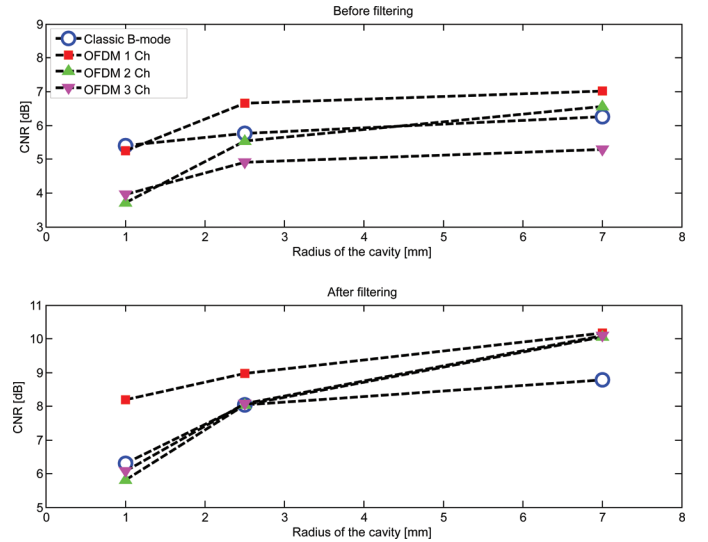


Fig. 5. Contrast-to-noise ratio as obtained with classic B-mode and parallel beamforming by means of OFDM with one, two, and three channels. Results before and after spatial filtering are shown.

echo imaging influences the axial resolution of the ultrasound image.

- 2) Increasing the number of beams transmitted in parallel results in a gradual deformation of the speckle pattern toward a stripe-like pattern. The speckle pattern is dependent on the transmitted frequency, and this deformation is most likely due to adjacent lines being formed with beams generated by ultrasound fields centered at a different center frequency. As shown in this paper, this deformation can be reduced by applying a simple spatial filtering.
- 3) Observing the CNR results for the PBT images, decreasing CNR values were obtained with both decreasing radius of the cavity and increasing the number of beams transmitted in parallel. This is due to interbeam interference. With PBT by means of OFDM, interbeam interference manifests itself with the appearance, along each line, of ghost echoes of a scatterer which are displaced from the position of the actual scatterer according to the delay applied between the beams, and is due to post-filtering residuals of adjacent beams [19]. Hence, the more beams are transmitted in parallel, the smaller the frequency separation between the beams, the higher the interference, and the lower the CNR. Moreover, CNR is lower for smaller cavities than for larger ones. Indeed, the ghost scatterers extend for a relatively larger portion of the cavity. As shown in this paper, simple spatial filtering can be applied to regularize the CNR when increasing the number of beams transmitted in parallel.
- 4) Both for the phantom and *in vivo* images, no special frequency-dependent attenuation compensation was needed. The same TGC settings were used for all the acquisition configurations, because the system allows only one TGC setting for each transmission/

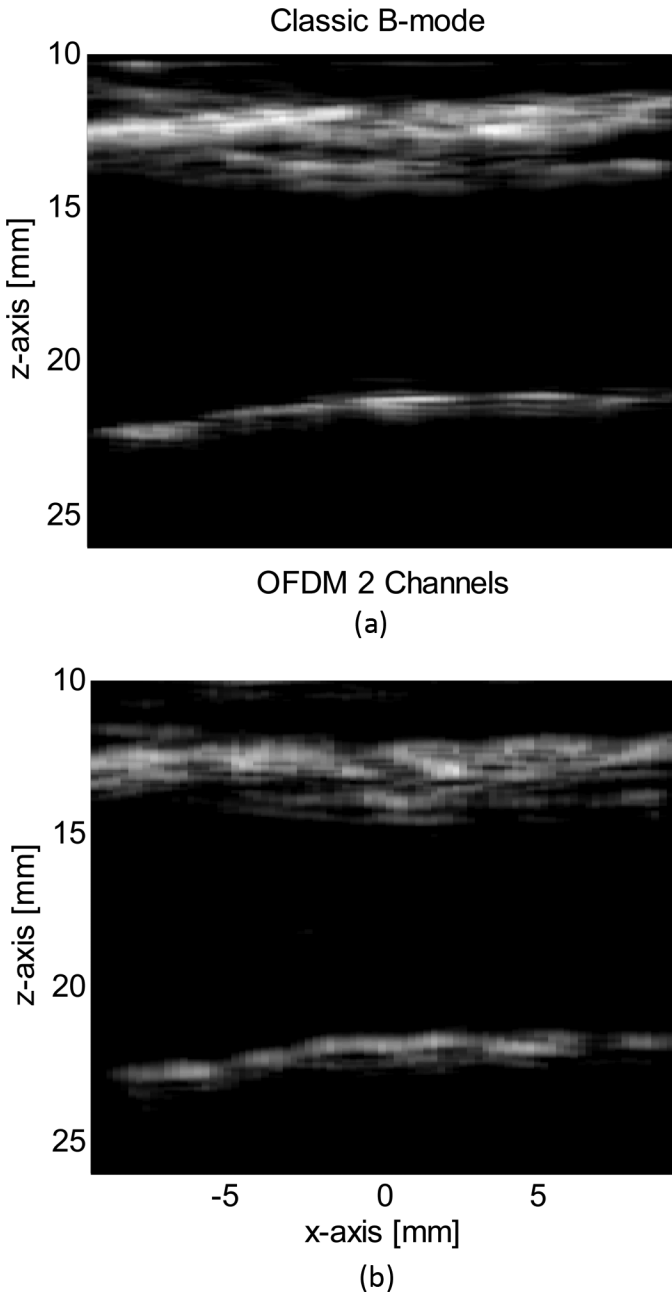


Fig. 6. Carotid artery tissue harmonic image as obtained with (a) classic B-mode and (b) parallel beamforming by means of OFDM. Spatial filtering applied. A 20-dB dynamic range is shown.

reception event. Even if the post-processing could be improved by selecting different TGC for each of the 3 transmit beams, this would not be feasible in a future real-time implementation.

- 5) In this paper, *in vitro* and *in vivo* tissue harmonic images obtained with PBT by means of OFDM were shown, achieving a gain in frame rate equal to three and two, respectively, when compared with classic B-mode tissue harmonic imaging. Ultimately, PBT by means of OFDM can be applied in combination with other PBT techniques based on the spatial distribution of the transmitted beams, e.g., to improve further the frame rate of cardiac ultrasonography.

V. CONCLUSION

In this paper, tissue harmonic images of an agarose phantom and carotid artery *in vivo*, as obtained with PBT by means of OFDM, were shown. These results confirm the applicability of this technique to ultrasonography as a means to improve the data acquisition rate. This technique may be combined with other PBT techniques based on the spatial distribution of the transmitted beams to provide a further boost to the achievable frame rate. When applied to cardiac ultrasonography, this can potentially lead to focused tissue harmonic ultrasound images at a frame rate up to 900 Hz [14]. This, and a comparison of the proposed method with other PBT techniques, will be the focus of future work.

ACKNOWLEDGMENTS

The authors thank Prof. P. Tortoli for facilitating the access to the lab facilities at the Laboratory of Microelectronics Systems Design, Università degli Studi di Firenze, Italy.

REFERENCES

- [1] R. Mallart and M. Fink, "Improved imaging rate through simultaneous transmission of several ultrasound beams," *Proc. SPIE*, vol. 1733, pp. 120–130, 1992.
- [2] E. D. Light, R. E. Davidsen, J. O. Fiering, T. A. Hruschka, and S. W. Smith, "Progress in two dimensional arrays for real time volumetric imaging," *Ultrason. Imaging*, vol. 20, no. 1, pp. 1–15, 1998.
- [3] D. P. Shattuck, M. D. Weishenker, S. W. Smith, and O. T. von Ramm, "Explososcan: A parallel processing technique for high speed ultrasound imaging with linear phased array," *J. Acoust. Soc. Am.*, vol. 75, no. 4, pp. 1273–1282, 1984.
- [4] S. W. Smith, H. G. Pavly, and O. T. von Ramm, "High-speed ultrasound volumetric imaging system. I. Transducer design and beam steering," *IEEE Trans. Ultrason. Ferroelectr. Freq. Control*, vol. 38, no. 2, pp. 100–108, 1991.
- [5] O. T. von Ramm, S. W. Smith, and H. G. Pavly, "High-speed ultrasound volumetric imaging system. II. Parallel processing and image display," *IEEE Trans. Ultrason. Ferroelectr. Freq. Control*, vol. 38, no. 2, pp. 109–115, 1991.
- [6] G. Montaldo, M. Tanter, J. Bercoff, N. Benech, and M. Fink, "Coherent plane wave compounding for very high frame rate ultrasonography and transient elastography," *IEEE Trans. Ultrason. Ferroelectr. Freq. Control*, vol. 56, no. 3, pp. 489–506, 2009.
- [7] L. Tong, H. Gao, H. F. Chio, and J. D'hooge, "Comparison of conventional parallel beamforming with plane wave and diverging wave imaging for cardiac applications: A simulation study," *IEEE Trans. Ultrason. Ferroelectr. Freq. Control*, vol. 59, no. 8, pp. 1654–1663, 2012.
- [8] T. Christopher, "Finite amplitude distortion-based inhomogeneous pulse echo ultrasonic imaging," *IEEE Trans. Ultrason. Ferroelectr. Freq. Control*, vol. 44, no. 1, pp. 125–139, 1997.
- [9] M. A. Averkiou, D. N. Roundhill, and J. E. Powers, "A new imaging technique based on the nonlinear properties of tissues," in *Proc. IEEE Ultrasonics Symp.*, 1997, pp. 1561–1566.
- [10] B. Ward, A. C. Baker, and V. F. Humphrey, "Nonlinear propagation applied to the improvement of resolution in diagnostic medical ultrasound equipment," *J. Acoust. Soc. Am.*, vol. 101, no. 1, pp. 143–154, 1997.
- [11] F. Tranquart, N. Grenier, V. Eder, and L. Pourcelot, "Clinical use of ultrasound tissue harmonic imaging," *Ultrasound Med. Biol.*, vol. 25, no. 6, pp. 889–894, 1999.

- [12] P. L. M. J. van Neer, M. G. Danilouchkine, M. D. Verweij, L. Demi, M. M. Voormolen, A. F. W. van der Steen, and N. de Jong, "Comparison of fundamental, second harmonic, and superharmonic imaging: A simulation study," *J. Acoust. Soc. Am.*, vol. 130, no. 5, pp. 3148–3157, 2011.
- [13] L. Tong, H. Gao, and J. D'hooge, "Multi-transmit beam forming for fast cardiac imaging—A simulation study," *IEEE Trans. Ultrason. Ferroelectr. Freq. Control*, vol. 60, no. 8, pp. 1719–1731, 2013.
- [14] L. Tong, A. Ramalli, R. Jasaityte, P. Tortoli, and J. D'hooge, "Multi-transmit beam forming for fast cardiac imaging—Experimental validation and in vivo application," *IEEE Trans. Med. Imaging*, vol. 33, no. 6, pp. 1205–1219, 2014.
- [15] B. Denarie, T. Bjastad, and H. Torp, "Multi-line transmission in 3-D with reduced crosstalk artifacts: A proof of concept study," *IEEE Trans. Ultrason. Ferroelectr. Freq. Control*, vol. 60, no. 8, pp. 1708–1718, 2013.
- [16] A. Drukarev, K. Konstantinides, and G. Seroussi, "Beam transformation techniques for ultrasonic medical imaging," *IEEE Trans. Ultrason. Ferroelectr. Freq. Control*, vol. 40, no. 6, pp. 717–726, 1993.
- [17] L. Demi, M. D. Verweij, and K. W. A. van Dongen, "Parallel transmit beamforming using orthogonal frequency division multiplexing applied to harmonic imaging—A feasibility study," *IEEE Trans. Ultrason. Ferroelectr. Freq. Control*, vol. 59, no. 11, pp. 2439–2447, 2012.
- [18] L. Demi and M. D. Verweij, "Nonlinear acoustics," in *Comprehensive Biomedical Physics*, Oxford, UK: Elsevier Science Ltd., 2014, ch. 2.16, pp. 387–399.
- [19] L. Demi, J. Viti, L. Kusters, F. Guidi, P. Tortoli, and M. Mischi, "Implementation of parallel transmit beamforming using orthogonal frequency division multiplexing—Achievable resolution and inter-beam interference," *IEEE Trans. Ultrason. Ferroelectr. Freq. Control*, vol. 60, no. 11, pp. 2310–2320, 2013.
- [20] E. Boni, L. Bassi, A. Dallai, F. Guidi, A. Ramalli, S. Ricci, R. Housden, and P. Tortoli, "A reconfigurable and programmable FPGA based system for non-standard ultrasound methods," *IEEE Trans. Ultrason. Ferroelectr. Freq. Control*, vol. 59, no. 7, pp. 1378–1385, 2012.
- [21] C. J. Teirlinck, R. A. Bezemer, C. Kollmann, J. Lubbers, P. R. Hoskins, K. V. Ramnarine, P. Fish, K. E. Fredeldt, and U. G. Schaarschmidt, "Development of an example flow test object and comparison of five of these test objects, constructed in various laboratories," *Ultrasonics*, vol. 36, no. 1–5, pp. 653–660, 1998.
- [22] T. Varghese and J. Ophir, "An analysis of elastographic contrast-to-noise ratio," *Ultrasound Med. Biol.*, vol. 24, no. 6, pp. 915–924, 1998.